scientific reports

Check for updates

OPEN

Improvement of low temperature carbon combustion catalyst characteristic caused by mixing Bi_2O_3 with Tl_2O_3

Susumu Nakayama

This study investigated the addition of various oxides to further improve the catalytic characteristics of Tl_2O_3, which offers a high carbon combustion catalytic capacity to lower the carbon combustion temperature of 660 °C by ~ 300 °C. Mixtures of carbon (2 wt%) with composite catalysts comprising 20 wt% Tl_2O_3–80wt% added oxide were analyzed using DSC. Bi_2O_3 offered the best improvement, where the exothermic peak temperatures for carbon combustion of carbon with various Tl_2O_3–*x* wt% Bi_2O_3 composites were lower than that of carbon with pure Tl_2O_3. Isothermal TG measurements were performed using a mixture of carbon and the Tl_2O_3—95 wt% Bi_2O_3 composite catalyst, where a 2 wt% weight loss (i.e. removal of all carbon) was achieved above 230 °C. A porous alumina filter was coated with the composite catalyst and carbon was deposited on the filter surface. The filter was held at constant temperatures under air flow, which confirmed that carbon was completely removed at 230 °C. This study demonstrated the potential for using these composite catalysts in self-cleaning particulate filters to decompose and eliminate fine particulate matter and diesel particulate matter generated from steelworks, thermal power plants, and diesel vehicles simply using the heat of the exhaust gas in a factory flue-gas stack or vehicle muffler.

Carbon-based fine particulate matter with a diameter of less than 2.5 μm (PM2.5) is generated from steelworks and thermal power plants that consume large amounts of coal. The environmental pollution associated with PM2.5 has become a major social problem[1–3]. The technologies typically used to eliminate PM2.5 include filtering, where multiple filters of different fineness values are used[4,5], and electrical removal, where positively or negatively charged fine particle droplets are sprayed[6,7]. However, these methods have serious drawbacks, including the need for regular cleaning and complex systems.

Diesel engines offer high energy efficiency and the suppression of carbon dioxide emission, but generate exhaust gas containing diesel particulate matter (DPM) associated with human health risks and environmental contamination[8,9]. In response, research has aimed to develop carbon combustion catalysts to eliminate DPM exhausted from diesel engines at lower temperatures than the current conventional catalysts[10–17]. For example, $La_{0.8}Cr_{0.9}Li_{0.1}O_3$[10], CeO_2–ZrO_2–Bi_2O_3[11], $La_{0.9}Rb_{0.1}CoO_3$[13], and $CeO_2/Pr_{4.8}Bi_{1.2}O_{11}$[14] catalysts have been reported. Exhaust gas from diesel cars can be controlled via the collection and elimination of DPM using a filter, where an oxidation catalyst is generally used. This technology has also been considered for the removal of PM2.5 originating from steelworks and thermal power plants.

Although the combustion temperature for pure carbon has been determined using differential scanning calorimetry (DSC) as 660 °C, this can be reduced to ~ 500 °C by adding copper oxide to the carbon[18]. The combustion temperature may be reduced by a further 50 °C when a complex oxide with rare-earth elements are used[19]. Specifically, a previous study found that the addition of yttrium-manganate led to an exothermic DSC peak at ~ 430 °C, which resulted in good carbon combustion properties[20]. In addition, a previous report on Tl_2O_3 observed explosive carbon combustion at ~ 300 °C when 5% or more carbon was mixed with thallium (III) oxide (Tl_2O_3) (**Fig. 1**) [21]. The video of explosive carbon combustion with sparks can be found in **Fig. 2 (Video Number—1)**. It should be noted that $Tl^{III}{}_2O_3$ is not poisonous, unlike $Tl^{I}{}_2SO_4$ and $Tl^{I}NO_3$. The application of Tl_2O_3 alone is not realistic because thallium is a rare and expensive metal. Thus, the development of Tl_2O_3 composites with other metal oxides is important.

Department of Applied Chemistry and Biotechnology, National Institute of Technology (KOSEN), Niihama College, 7-1 Yagumo-cho, Niihama-shi, Ehime 792-8580, Japan. email: s.nakayama@niihama-nct.ac.jp

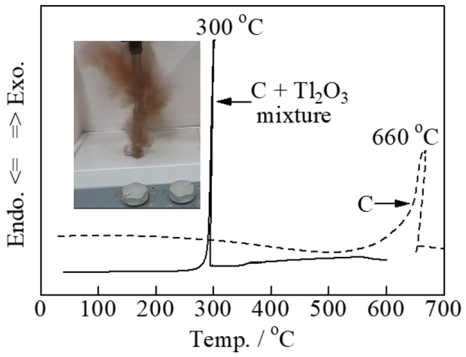

Figure 1. DSC curves of carbon black (5 wt%) mixed with a pure Tl_2O_3 catalyst. Inset is a digital photograph of explosive carbon combustion.

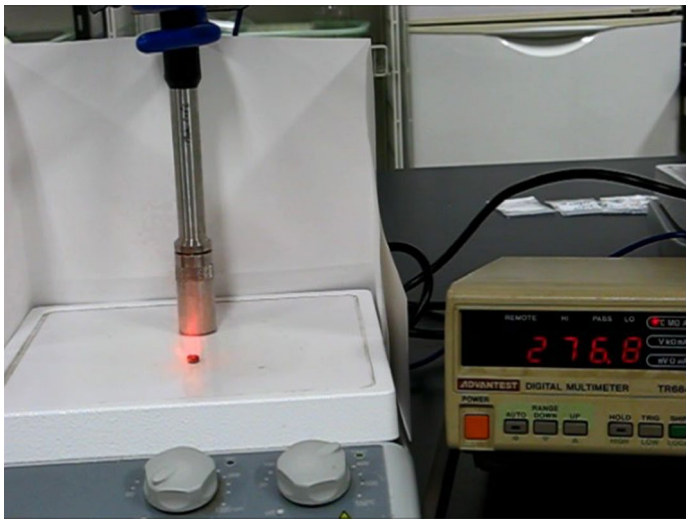

Figure 2. (Video Number—1) Video showing explosive carbon combustion with sparks.

This study aimed to composite Tl_2O_3 with other metal oxides that can supply oxygen in the lattice. The composites were evaluated based on their ability to maintain and improve the catalytic properties of Tl_2O_3 for low-temperature carbon combustion while reducing the amount of Tl_2O in the catalyst. Furthermore, the collection of PM2.5 and DPM from exhaust gas was explored using porous ceramic filters coated with the catalytic composites for low-temperature carbon combustion. The filters show promise for applications in the flue-gas stacks of factories or on the muffler of cars. The performance of the self-cleaning type particulate filter for the collection of PM2.5 and DPM was demonstrated experimentally, where the carbon can subsequently be decomposed and removed simply due to the heat of the exhaust gas.

Results and discussion

Carbon combustion characteristics of the Tl_2O_3–80 wt% added oxide. Tl_2O_3 offers excellent carbon combustion properties, and was mixed with both general single oxides, namely CeO_2, α-Al_2O_3, ZrO_2, TiO_2, Bi_2O_3, Pr_6O_{11}, Cr_2O_3, and MnO_2, and complex oxides with ionic conductivity, namely $(Bi_2O_3)_{0.75}(Y_2O_3)_{0.25}$, $(CeO_2)_{0.8}(Gd_2O_3)_{0.2}$, $La_{9.7}Si_6O_{26.55}$, and $Pr_{4.8}Bi_{1.2}O_{11}$. Further, $YMnO_3$ was also investigated due to its promising catalytic properties for carbon combustion. The carbon combustion properties of the mixed composite catalysts were improved compared to that of a pure Tl_2O_3 catalyst when added to 2 wt% carbon (**Fig. 3**). Specifically, the six oxides that led to improved carbon combustion were Bi_2O_3, Pr_6O_{11}, $(CeO_2)_{0.8}(Gd_2O_3)_{0.2}$, $(Bi_2O_3)_{0.75}(Y_2O_3)_{0.25}$, $La_{9.7}Si_6O_{26.55}$, and $Pr_{4.8}Bi_{1.2}O_{11}$, where Bi_2O_3 had the largest effect. For comparison, the carbon combustion properties of the Bi_2O_3, Pr_6O_{11}, $(CeO_2)_{0.8}(Gd_2O_3)_{0.2}$, $(Bi_2O_3)_{0.75}(Y_2O_3)_{0.25}$, $La_{9.7}Si_6O_{26.55}$, and $Pr_{4.8}Bi_{1.2}O_{11}$ catalysts with added to 2 wt% carbon are shown in **Fig. 4**. The carbon combustion temperature for all samples was higher than 380 °C. However, the remaining eight oxides did not lead to improved carbon combustion properties (2 wt% carbon), namely CeO_2, α-Al_2O_3, ZrO_2, MnO_2, TiO_2, Cr_2O_3, $(ZrO_2)_{0.92}(Y_2O_3)_{0.08}$, and $YMnO_3$, where the carbon combustion performance was reduced compared to that of pure Tl_2O_3 (**Fig. 5**).

Carbon combustion characteristics of the Tl_2O_3 −Bi_2O_3 system. *Carbon combustion characteristics of Tl_2O_3–x wt% Bi_2O_3 (x = 5–95).* The addition of Bi_2O_3 led to the best carbon combustion properties (2 wt%

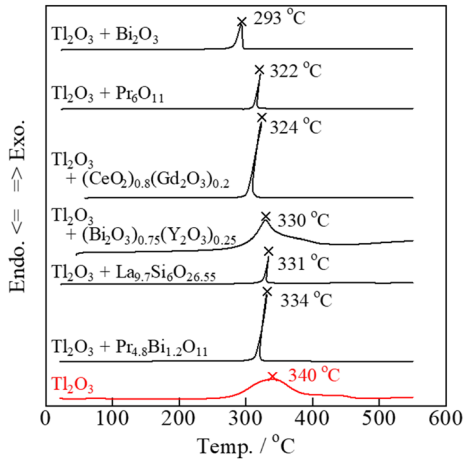

Figure 3. DSC curves of carbon black (2 wt%) mixed with the various Tl_2O_3—80 wt% added oxide composite catalysts.

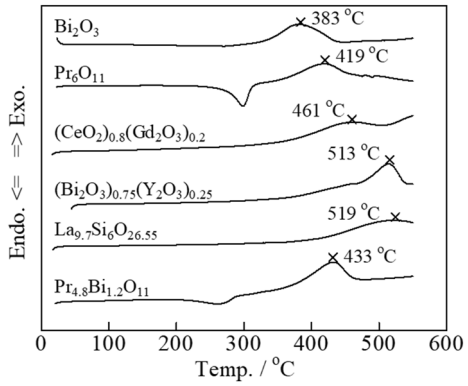

Figure 4. DSC curves of carbon black (2 wt%) mixed with the various oxide catalysts.

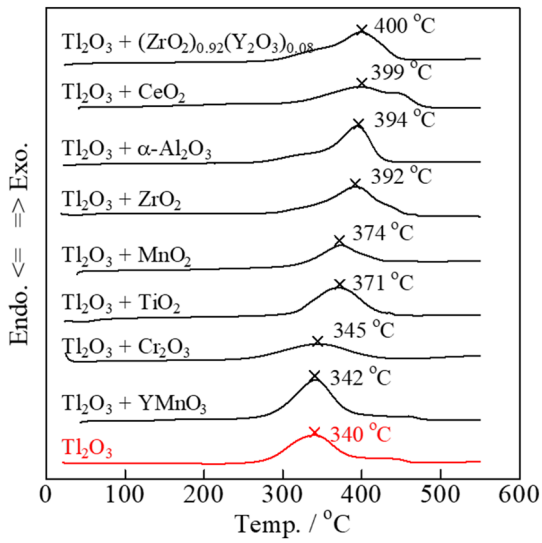

Figure 5. DSC curves of carbon black (2 wt%) mixed with the various Tl_2O_3—80 wt% added oxide composite catalysts.

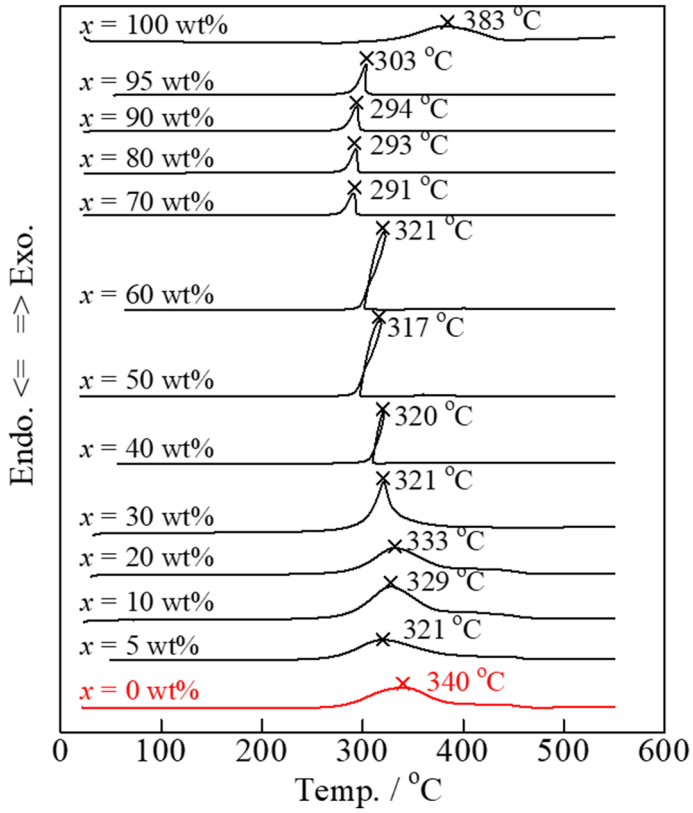

Figure 6. DSC curves of carbon black (2 wt%) mixed with the various Tl_2O_3— *x* wt% Bi_2O_3 (*x* = 0–100) composite catalysts.

carbon) among the various oxides added to Tl_2O_3. Thus, the relationship between the proportion of Bi_2O_3 in the composite catalyst and the carbon combustion properties was investigated. DSC analysis of the Tl_2O_3—*x* wt% Bi_2O_3 (*x* = 0—100) composite catalyst mixed with 2 wt% carbon was compared to Tl_2O_3—*x* wt% Bi_2O_3 (*x* = 0—100) with no added carbon to determine the carbon combustion performance (**Fig. 6**). The DSC exothermal peaks of carbon combustion (2 wt% carbon) with pure Tl_2O_3 and Bi_2O_3 catalysts were observed at 340 and 383 °C, respectively. All of the Tl_2O_3—*x* wt% Bi_2O_3 composite catalysts exhibited lower exothermal peak temperatures for carbon combustion compared to that of pure Tl_2O_3. In particular, the samples with *x* values of 70, 80, and 90 wt% exhibited exothermal peak temperatures during carbon combustion (2 wt% carbon) of 300 °C or less, which was indicative of excellent properties.

Carbon combustion characteristics of thermal-treated Tl_2O_3–95 wt% Bi_2O_3. Applications of carbon combustion catalysts often involve environments associated with the exposure to temperatures of ~ 500 °C. Carbon (2 wt%) was mixed with the Tl_2O_3—95 wt % Bi_2O_3 catalyst, and was either left unheated or heat-treated at 200, 300, 400, and 500 °C. DSC analysis revealed minimal changes in the temperature of the exothermal peaks due to carbon combustion (**Fig. 7**). Thus, heat treatments of 500 °C or below had a minimal effect on the carbon combustion properties of Tl_2O_3—95 wt% Bi_2O_3. The formation of new phases in addition to Tl_2O_3 and Bi_2O_3 was evaluated during XRD analysis of the Tl_2O_3—95 wt% Bi_2O_3 catalyst after heating at 500 °C (**Fig. 8**). All of the XRD peaks observed at 2θ values of 20° to 60° were attributed to Tl_2O_3 and Bi_2O_3, thus the formation of complex oxides (e.g. Tl_3BiO_3) was not observed.

Carbon combustion mechanism of the Tl_2O_3–Bi_2O_3 system. Thallium(III) oxide (Tl_2O_3) powder containing 5 wt%-carbon was placed on a porcelain dish (Nikkato Co., CW-1). When the mixture was gradually heated, explosive reaction (combustion) occurred around 300 ℃ and the reaction products were scattered (**Fig. 1**). A very small amount of brown residue remained on the porcelain dish was subjected to the XRD measurement. The XRD pattern measured immediately after the explosive reaction showed a weak peak attributable to Tl_2O around $2\theta = 31°$ in addition to peaks attributed to Tl_2O_3 (**Fig. 9(a)**), whereas the peak attributable to Tl_2O disappeared in the XRD pattern measured after further heating of the residue in air at 300 ℃ (**Fig. 9(b)**). As generally known, porcelain dish itself shows no diffraction peak (**Fig. 9(c)**). In order to investigate the cause of this disappearance, the TG–DTA measurement was performed for Tl_2O (Kojundo Chemical Lab. Co., Ltd., 98% purity) in an air stream. **Figure 10** shows an exothermic peak with a maximum at 200 ℃ resulting in an increase in weight which corresponds to the formation of Tl_2O_3 by the oxidation of Tl_2O. In fact, it was confirmed that the sample obtained by igniting the Tl_2O powder at 200 ℃ in a platinum crucible exhibited the XRD pattern of Tl_2O_3 and

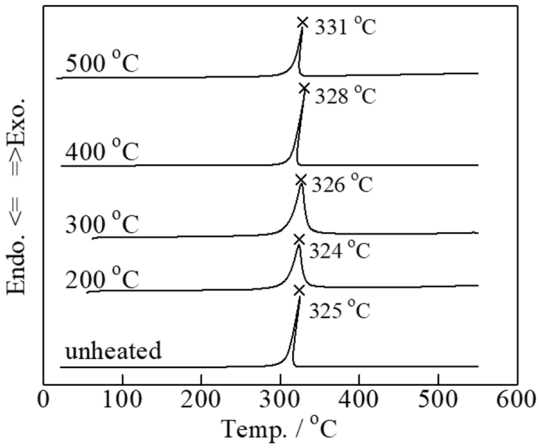

Figure 7. DSC curves of carbon black (2 wt%) mixed with Tl_2O_3—95 wt%Bi_2O_3 and either left unheated or heat-treated at 200, 300, 400, and 500 °C for 2 h.

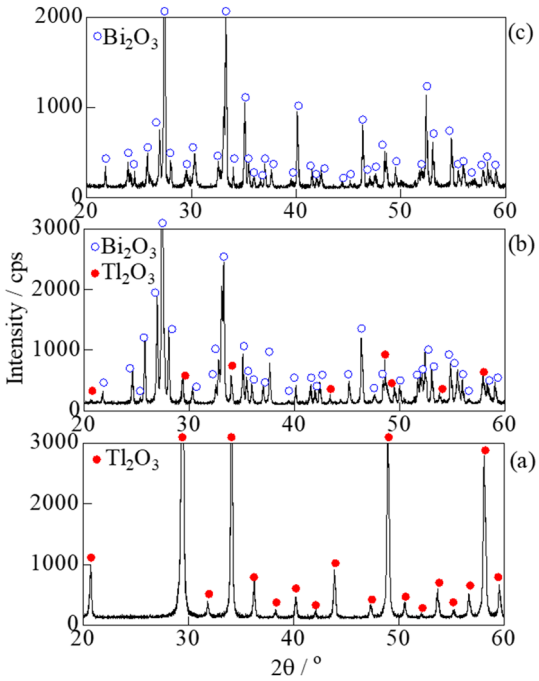

Figure 8. XRD analysis of (a) Tl_2O_3, (b) Tl_2O_3—95 wt% Bi_2O_3, and (c) Bi_2O_3 after heat-treatment at 500 ℃ for 2 h.

no peaks attributable to Tl_2O. From these results, the carbon combustion mechanism on Tl_2O_3 can be presumed as follows:

$Tl_2O_3 + 2C \rightarrow 2\,Tl_2O + 2CO$.

$2CO + O_2 \rightarrow 2CO_2$.

$Tl_2O + O_2 \rightarrow Tl_2O_3$.

At first, the lattice oxide ions in Tl_2O_3 are released for the oxidation of carbon to form CO and Tl_2O. Then CO molecules immediately react with the surrounding oxygen at elevated temperature to give CO_2 molecules. The Tl_2O is also oxidized to Tl_2O_3 by the oxygen in air at 200 ℃ or above (300 ℃ in the present experimental condition) as shown in **Fig. 10**. Thus, Tl_2O_3 functions as a combustion catalyst for carbon.

The carbon combustion mechanism of the Tl_2O_3—Bi_2O_3 system was proposed. Although the system comprised a smaller proportion of Tl_2O_3 compared to Bi_2O_3, the lattice oxygen in Tl_2O_3 was used for carbon combustion. The lattice defects of oxygen in Tl_2O_3 caused by carbon combustion were immediately recovered by the lattice oxygen in Bi_2O_3 (**Fig. 11**). Therefore, the catalytic functioning for carbon combustion was continuously maintained in Tl_2O_3. Furthermore, the high oxygen desorption properties of Bi_2O_3 likely enhanced the carbon combustion properties of Tl_2O_3. SEM observation and EDS mapping (Tl and Bi) of the Tl_2O_3—95 wt% Bi_2O_3 powder

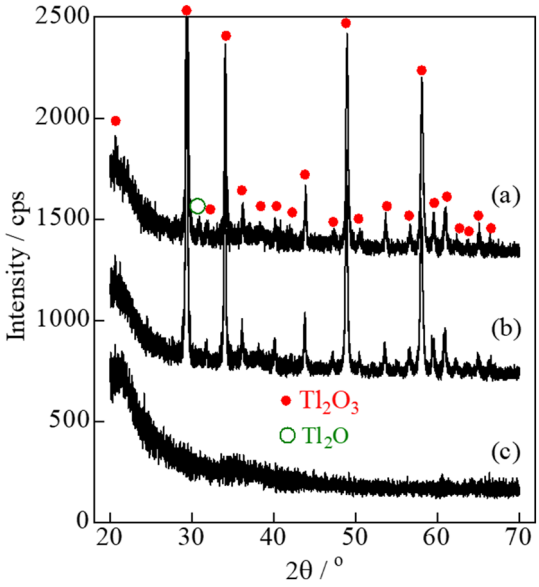

Figure 9. XRD analysis of the surface of porcelain dish. (a) Brown residue after reacting carbon black (5 wt%) mixed with Tl_2O_3 explosively at 300 ℃, (b) thermal-treated product after further heating of the brown residue in air at 300 ℃, and (c) an unused porcelain dish.

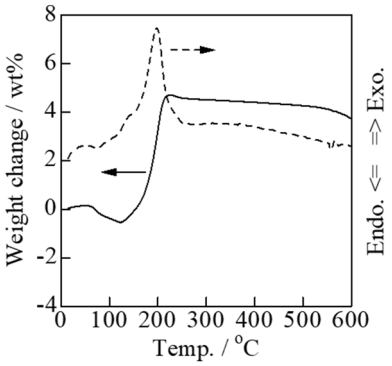

Figure 10. TG–DTA curves of Tl_2O.

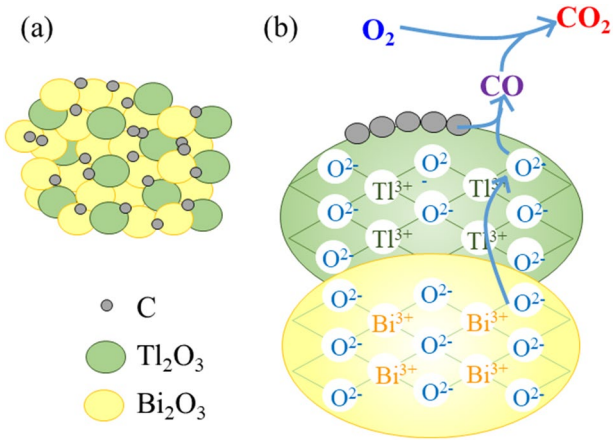

Figure 11. Schematic illustrations of (a) the carbon and Tl_2O_3—Bi_2O_3 mixture and (b) the Tl_2O_3-modified Bi_2O_3-based carbon combustion catalyst and its oxygen transfer mechanism during carbon oxidation. The particle size of carbon is 14 nm (manufacturer data), and of Tl_2O_3 and Bi_2O_3 is 0.5 to 3 μm (SEM observations).

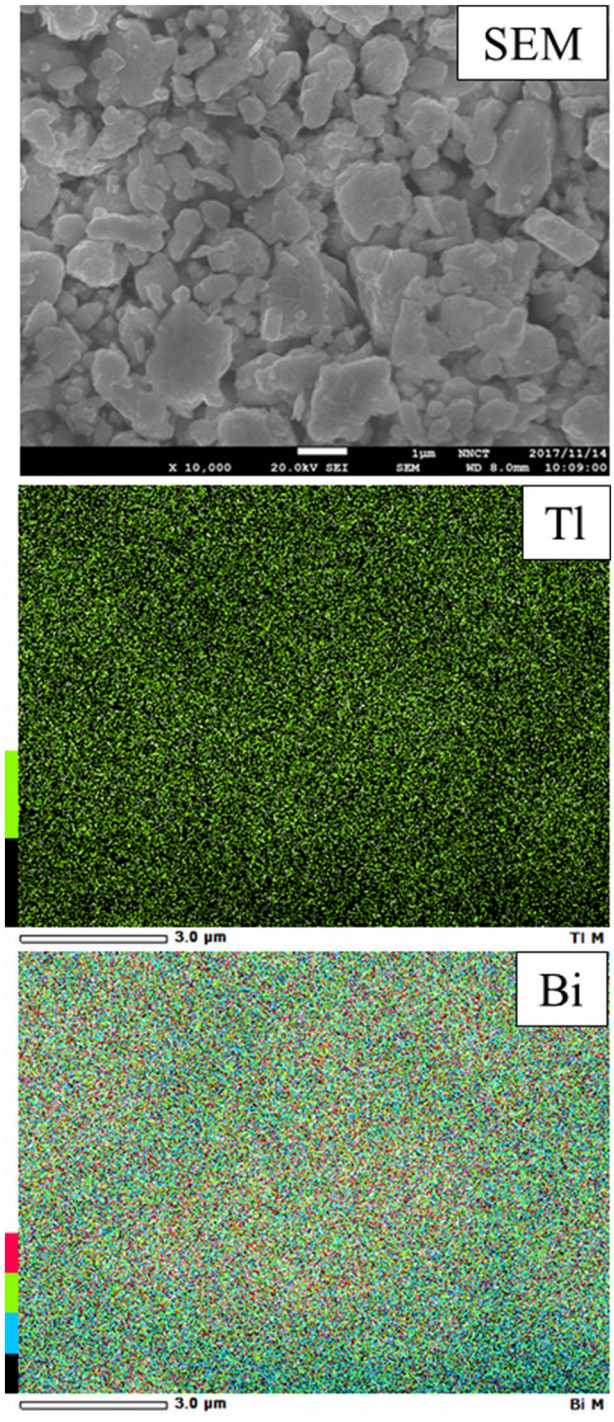

Figure 12. SEM image and EDS elemental mapping images of the Tl_2O_3—95 wt% Bi_2O_3 composite catalyst.

confirmed that the particle size of the Tl_2O_3 and Bi_2O_3 powders was ~ 0.5 to 3 μm, which were homogeneously distributed (**Fig. 12**).

Carbon combustion characteristics of Tl_2O_3– x wt% Bi_2O_3 (x = 95–99.5). Tl_2O_3 costs about ten times more than Bi_2O_3, thus the cost must be minimized to facilitate practical implementation. The carbon combustion performance was evaluated as the proportion of Bi_2O_3 was increased above 95 wt% (**Fig. 13**). A large exothermal peak due to carbon combustion was observed up to 99 wt%, but the temperature was slightly higher at 336 °C. These findings indicated that the carbon combustion catalytic function of Tl_2O_3 was maintained at levels of only 1 wt%.

Actual carbon combustion is assumed to begin at the rising temperature of the exothermal peak. The temperature at which real carbon combustion initiated and progressed was determined based on isothermal TG analysis of the Tl_2O_3—95 wt% Bi_2O_3 composite catalyst. The sample was heated in an air stream to either 230,

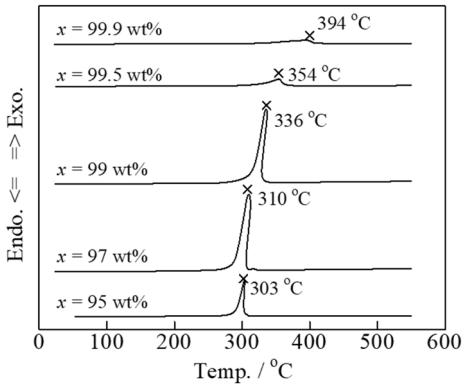

Figure 13. DSC curves of carbon black (2 wt%) mixed with the various Tl_2O_3– x wt%Bi_2O_3 (x = 95–99.9) composite catalysts.

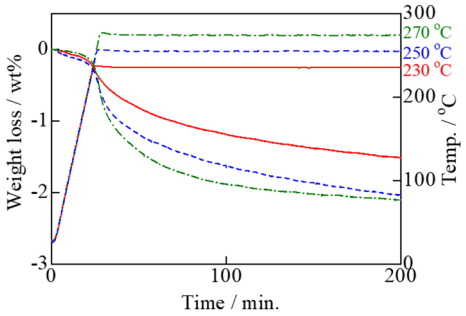

Figure 14. Isothermal TG analysis of carbon black (2 wt%) mixed with the Tl_2O_3–95 wt%Bi_2O_3 composite catalyst at constant temperatures of 230, 250, and 270 °C for 3 h.

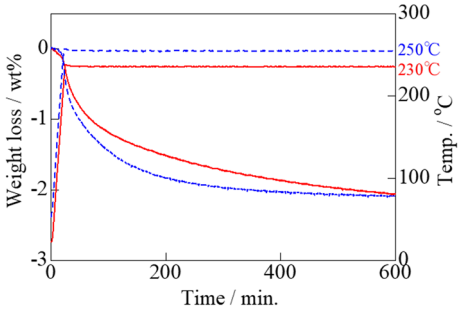

Figure 15. Isothermal TG analysis of carbon black (2 wt%) mixed with the Tl_2O_3–95 wt% Bi_2O_3 composite catalyst at constant temperatures of 230 and 250 °C for 10 h.

250, or 270 °C, where the weight loss was measured as the sample was held at the respective temperature. The amount of carbon added was 2 wt%, thus the weight loss of 2 wt% after 3 h at 270 °C corresponded to the combustion of all added carbon (**Fig. 14**). Further, a 2 wt% weight loss was confirmed at 10 h when heated at 230 and 250 °C (**Fig. 15**). However, only a ~ 1 wt% weight loss was achieved after heating at 200 °C for 20 h. These results indicated that the carbon combustion reaction occurred at temperatures higher than ~ 230 °C.

Carbon combustion using an alumina filter coated with Tl_2O_3–95wt%Bi_2O_3. The combustion of carbon on a catalyst-supported alumina filter was demonstrated experimentally using the set-up shown in **Fig. 16**. Carbon in the form of candle soot was deposited onto the catalyst-supported alumina filter, and the filter was held at constant temperatures of 250, 240, 230, and 220 °C (**Fig. 17**). Complete removal of the soot via carbon combustion required ~ 68, ~ 123, and ~ 165 h at 250, 240, and 230 °C, respectively. The soot was not be completely removed at 220 °C after 216 h.

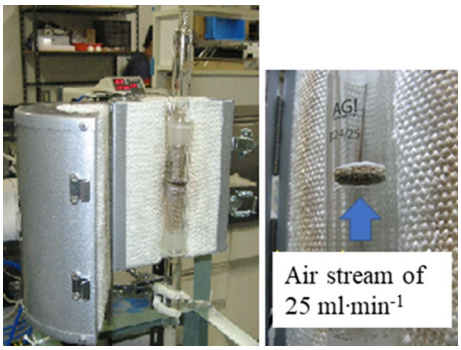

Figure 16. Experimental set-up for evaluating the carbon combustion characteristics of a porous alumina filter coated by the carbon combustion catalyst.

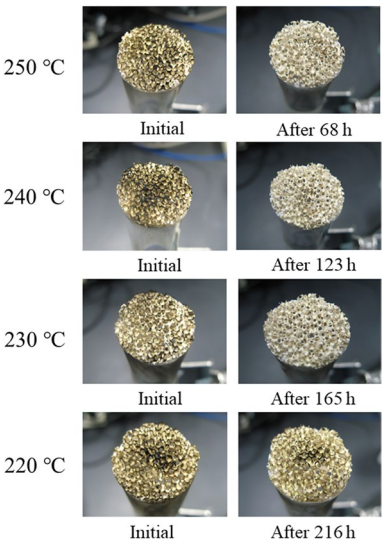

Figure 17. Carbon combustion using the coated porous alumina filter at 220 to 250 °C in an air stream of 25 ml·min^{-1}.

These results demonstrated that PM2.5 and DPM in exhaust gas could potentially be collected and decomposed using porous ceramic filters coated with the low-temperature PM combustion Tl_2O_3—Bi_2O_3 catalytic system proposed in this study. This is expected to lead to the development of self-cleaning PM filters capable of decomposing and eliminating PM2.5 and DPM simply using the heat of the exhaust gas from a factory flue-gas stack or diesel vehicle muffler.

Conclusions

The carbon combustion temperature of 660 °C can be reduced to 300 °C due to the catalytic effect of Tl_2O_3. This excellent carbon combustion catalytic property of Tl_2O_3 was further improved by mixing Tl_2O_3 with various oxides. Further, a porous ceramic filter was coated with the proposed Tl_2O_3-system catalyst to demonstrate its promising catalytic performance. Based on the findings of this study, the following conclusions can be drawn:

1. DSC analysis of the Tl_2O_3—80wt% added oxide composite catalysts in the presence of 2 wt% carbon revealed that carbon combustion was enhanced by the addition of Bi_2O_3, Pr_6O_{11}, $(CeO_2)_{0.8}(Gd_2O_3)_{0.2}$, $(Bi_2O_3)_{0.75}(Y_2O_3)_{0.25}$, $La_{9.7}Si_6O_{26.55}$, and $Pr_{4.8}Bi_{1.2}O_{11}$, where Bi_2O_3 exhibited a particularly outstanding performance. However, some of the oxides, including CeO_2, α-Al_2O_3, ZrO_2, MnO_2, TiO_2, Cr_2O_3, $(ZrO_2)_{0.92}(Y_2O_3)_{0.08}$, and $YMnO_3$, compromised the carbon combustion properties of Tl_2O_3.
2. The temperature of the exothermal peak due to carbon combustion (2 wt% carbon) during DSC analysis of the Tl_2O_3—x wt% Bi_2O_3 (x = 5—95) composite catalysts was reduced compared to that of pure Tl_2O_3. The best performance was observed at x values of 70, 80, and 90 wt%, where the temperature of the heat generation peak for carbon combustion was below 300 °C. Furthermore, a large exothermal peak was even observed at an x value of 99 wt%, but the temperature was ~ 336 °C.

3. Isothermal TG analysis of the Tl_2O_3—95 wt% Bi_2O_3 composite catalyst with 2 wt% carbon led to a weight loss of ~ 2 wt% at 230 °C and higher, which was indicative of complete carbon combustion. An alumina filter was coated with the Tl_2O_3—95wt%Bi_2O_3 catalyst and exposed to carbon in the form of candle soot. Holding the coated filter at 220 to 250 °C confirmed that carbon was completely combusted at 230 °C and higher.

Methods

Sample preparation. *Tl_2O_3 and various oxide mixtures.* Tl_2O_3 powder (2 g) was wet-mixed with various oxide powders (8 g), including CeO_2, α-Al_2O_3, ZrO_2, TiO_2, Bi_2O_3, Pr_6O_{11}, Cr_2O_3, MnO_2, $(ZrO_2)_{0.92}(Y_2O_3)_{0.08}$, $(Bi_2O_3)_{0.75}(Y_2O_3)_{0.25}$, $(CeO_2)_{0.8}(Gd_2O_3)_{0.2}$, $La_{9.7}Si_6O_{26.55}$, $Pr_{4.8}Bi_{1.2}O_{11}$, or $YMnO_3$, in deionized water using a planetary ball mill (Fritsch Co., Pulverisette 6) for 2 h. The mixtures were dried at 100 °C to obtain composites comprising Tl_2O_3–80 wt% added oxide.

Tl_2O_3 and Bi_2O_3 mixture. Mixtures of Tl_2O_3 with varying Bi_2O_3 contents (0.5—99.9 wt%) were prepared from Tl_2O_3 (Kojundo Chemical Lab. Co., Ltd., 99.9% purity) and Bi_2O_3 (Kisan Kinzoku Chemicals Co.,Ltd., 99.9% purity) powders. The Tl_2O_3 and Bi_2O_3 powder mixtures (10 g) were wet-mixed in deionized water using a planetary ball mill for 3 h and dried at 100 °C to give composites comprising Tl_2O_3–x wt% Bi_2O_3 (x = 0.5–99.9).

Characterization. The Tl_2O_3–80 wt% added oxide powders were analyzed using X-ray diffraction (XRD, Rigaku Co., MiniFlex II) in the 2θ range of 20° to 60° using $CuK_{\alpha 1}$. The Tl_2O_3—95 wt% Bi_2O_3 powder was observed and analyzed using scanning electron microscopy (SEM, Jeol Ltd., JSM-6510LA) with an energy dispersive spectroscopy (EDS) detector (Jeol Ltd., JED-2300).

The carbon combustion characteristics were evaluated by adding 2 wt% carbon black (Tokai Carbon Co., Ltd., Toka Black # 8500/F; average particle size = 14 nm; N_2 adsorption specific surface area = 290 $m^2 \cdot g^{-1}$) to the Tl_2O_3–80 wt% added oxide powders and mixing thoroughly in an agate mortar for 1 to 2 min. The mixture (10 mg) was transferred to a platinum pan for differential scanning calorimetry (DSC) analysis (DSC8230; Rigaku Co.) between room temperature and 600 °C at a heating rate of 10 °C $\cdot min^{-1}$ in a 20 mL $\cdot min^{-1}$ air stream. The temperature of the DSC exothermic peak was used as the carbon combustion temperature. A mixture of 2 wt% carbon and Tl_2O_3—95 wt%Bi_2O_3 powder was prepared in the same manner, and thermogravimetric (TG) analysis (TG8120; Rigaku Co.) was conducted under isothermal conditions for 3 to 20 h at 200, 230, 250, and 270 °C at a heating rate of 10 °C $\cdot min^{-1}$ in a 20 mL $\cdot min^{-1}$ air stream.

A ceramic filter coated with the Tl_2O_3—95 wt% Bi_2O_3 composite catalyst was prepared. The Tl_2O_3—95wt%Bi_2O_3 powder was dispersed in deionized water and coated on a porous Al_2O_3 ceramic foam filter (Shinagawa Fine Ceramics Co., Ltd., number of cells: 25–30 pieces/inch, φ20mm × t3mm) via a dipping method. The filter was fixed on a glass tube using an inorganic adhesive, and soot was deposited on the outer surface of the filter using a candle flame. The filter was transferred to a mantle heater furnace to evaluate its carbon decomposition and elimination performance. The condition of the soot deposited on the filter was observed every few hours under an air stream of 25 mL $\cdot min^{-1}$ from 200 to 270 °C provided by an air pump.

Received: 27 January 2021; Accepted: 19 March 2021
Published online: 05 May 2021

References

1. Liang, C.-S., Duan, F.-K., He, K.-B. & Ma, Y.-L. Review on recent progress in observations, source identifications and countermeasures of PM2.5, *Environment International* **86**, 150–170 https://doi.org/10.1016/j.envint.2015.10.016 (2016).
2. Li, G., Fang, C. & He, S. The influence of environmental efficiency on PM2.5 pollution: Evidence from 283 Chinese prefecture-level cities, *Science of the Total Environment* **748**, 141549 https://doi.org/10.1016/j.scitotenv.2020.141549 (2020).
3. Xie, X., Ai, H. & Deng, Z. Impacts of the scattered coal consumption on PM2.5 pollution in China, *Journal of Cleaner Production* **245**, 118922 https://doi.org/10.1016/j.jclepro.2019.118922 (2020).
4. Zhou, F., Diao, Y., Wang, R., Yang, B. & Zhang, T. Experimental study on PM2.5 removal by magnetic polyimide loaded with cobalt ferrate, *Energy and Built Environment* **1**, 404–409 https://doi.org/10.1016/j.enbenv.2020.04.009 (2020).
5. Yang, X., Pu, Y., Zhang, Y., Liu, X., Li, J., Yuan, D. & Ning, X. Multifunctional composite membrane based on $BaTiO_3$@PU/PSA nanofibers for high-efficiency PM2.5 removal, *Journal of Hazardous Materials* **391**, 122254 https://doi.org/10.1016/j.jhazmat.2020.122254 (2020).
6. Jaworek, A., Marchewicz, A., Sobczyk, A. T., Krupa, A. & Czech, T. Two-stage electrostatic precipitators for the reduction of PM2.5 particle emission, *Progress in Energy and Combustion Science* **67**, 206–233 https://doi.org/10.1016/j.pecs.2018.03.003 (2018).
7. Bin, H., Yang, Y., Lei, Z., Ao, S., Cai, L., Linjun, Y. & Roszak, S. Experimental and DFT studies of PM2.5 removal by chemical agglomeration, *Fuel* **212**, 27–33 https://doi.org/10.1016/j.fuel.2017.09.121 (2018).
8. Chen, C. *et al.* Study of the characteristics of PM and the correlation of soot and smoke opacity on the diesel methanol dual fuel engine. *Appl. Therm. Eng.* **148**, 391–403. https://doi.org/10.1016/j.applthermaleng.2018.11.062 (2019).
9. Nabi, M. N., Rasul, M. G. & Brown, R. J. Notable reductions in blow-by and particle emissions during cold and hot start operations from a turbocharged diesel engine using oxygenated fuels. *Fuel Process. Technol.* **203**, 106394. https://doi.org/10.1016/j.fuproc.2020.106394 (2020).
10. Russo, N., Fino, D., Saracco, G. & Specehia, V. Studies on the redox properties of chromite perovskite catalysts for soot combustion. *J. Catal.* **229**, 459–469. https://doi.org/10.1016/j.jcat.2004.11.025 (2005).
11. Masui, T., Minami, K., Koyabu, K. & Imanaka, N. Synthesis and characterization of new promoters based on CeO_2–ZrO_2–Bi_2O_3 for automotive exhaust catalysts. *Catal. Today* **117**, 187–192. https://doi.org/10.1016/j.cattod.2006.05.015 (2006).
12. Krishna, K., Lopez, A. B., Makkee, M. & Moulijn, J. A. Potential rare earth modified CeO_2 catalysts for soot oxidation: I. Characterisation and catalytic activity with O_2, *Applied Catalysis B: Environmental* **75**, 189–200 https://doi.org/10.1016/j.apcatb.2007.04.010 (2007).
13. Russo, N., Furfori, S., Fino, D., Saracco, G. & Specchia, V. Lanthanum cobaltite catalysts for diesel soot combustion. *Appl. Catal. B* **83**, 85–95. https://doi.org/10.1016/j.apcatb.2008.02.006 (2008).

14. Harada, K., Oishi, T., Hamamoto, S. & Ishihara, T. Lattice oxygen activity in Pr- and La-doped CeO_2 for low-temperature soot oxidation. *The Journal of Physical Chemistry C* **118**, 559–568. https://doi.org/10.1021/jp410996k (2014).
15. Wang, L., Fang, S., Feng, N., Wan, H. & Guan, G. Efficient catalytic removal of diesel soot over Mg substituted $K/La_{0.8}Ce_{0.2}CoO_3$ perovskites with large surface areas, *Chemical Engineering Journal* **293**, 68–74 https://doi.org/10.1016/j.cej.2016.02.038 (2016).
16. Lee, C., Shul, Y.-G. & Einaga, H. Silver and manganese oxide catalysts supported on mesoporous ZrO_2 nanofiber mats for catalytic removal of benzene and diesel soot. *Catal. Today* **281**, 460–466. https://doi.org/10.1016/j.cattod.2016.05.050 (2017).
17. Montini, T., Melchionna, M., Monai, M. & Fornasiero, P. Fundamentals and Catalytic Applications of CeO_2-Based Materials. *Chem. Rev.* **116**, 5987–6041. https://doi.org/10.1021/acs.chemrev.5b00603 (2016).
18. Nakayama, S., Kondo, S., Naka, T. & Sakamoto, M. Carbon oxidation activity of complex oxides (Part 1) RE_2CuO_4 (RE=La-Gd) and $RE_2Cu_2O_5$ (RE=Dy-Yb, Y). *J. Ceram. Soc. Jpn.* **119**, 961–964. https://doi.org/10.2109/jcersj2.119.961 (2011).
19. Nakayama, S., Tokunaga, R., Shiomi, M. & Naka, T. Carbon oxidation activity of complex oxides (Part 2) Characteristics of $La_{0.9}Ag_{0.1}FeO_\alpha$ synthesized at low temperature using co-precipitation method, *Journal of the Ceramic Society of Japan* **121**, 95–99 https://doi.org/10.2109/jcersj2.121.95 (2013).
20. Nakayama, S. *et al.* Carbon oxidation characteristics of yttrium manganate catalyst prepared via urea decomposition. *Ceram. Int.* **43**, 8538–8542. https://doi.org/10.1016/j.ceramint.2017.03.186 (2017).
21. Nakayama, S. & Sakamoto, M. High oxidation activity of thallium oxide for carbon combustion. *Thermochim. Acta* **647**, 81–85. https://doi.org/10.1016/j.tca.2016.12.005 (2017).

Acknowledgements

We would like to thank the direct contributions from the following students: Megumi Aibara, Yuri Akiduki, and Chiaki Umakoshi. Also, we would like to thank the Comprehensive Support Programs for Creation of Regional Innovation Science and Technology Incubation Program in Advanced Regions from Japan Science and Technology Agency (JST), the Grant of Steel Foundation for Environmental Protection Technology, and Editage (www.editage.com) for English language editing.

Author contributions

Corresponding author wrote all manuscript text and prepared all figures.

Competing interests

The author declares no competing interests.

Additional information

Correspondence and requests for materials should be addressed to S.N.

Reprints and permissions information is available at www.nature.com/reprints.

Publisher's note Springer Nature remains neutral with regard to jurisdictional claims in published maps and institutional affiliations.